Techno-Economic Modeling of Floating Wind Farms

Montes, Ariadna; Fournely, David; Sørensen, Jens N.; Larsen, Gunner C.

Published in:
Energies

Link to article, DOI:
10.3390/en18040967

Publication date:
2025

Document Version
Publisher's PDF, also known as Version of record

energies

MDPI

Article

Techno-Economic Modeling of Floating Wind Farms

Ariadna Montes [1], David Fournely [1], Jens N. Sørensen [2,*] and Gunner C. Larsen [3]

[1] Copenhagen Energy, Bag Elefanterne 1, 1799 Copenhagen, Denmark; amg@copenhagen-energy.com (A.M.); dpf@copenhagen-energy.com (D.F.)
[2] DTU Wind and Energy Systems, Technical University of Denmark, Nils Koppels Allé, bldg. 403, 2800 Lyngby, Denmark
[3] DTU Wind and Energy Systems, Technical University of Denmark, Risø Campus, Frederiksborgvej 399, bldg. 114, 4000 Roskilde, Denmark; gula@dtu.dk
* Correspondence: jnso@dtu.dk

Abstract: A simple techno-economic model for determining wind power production and costs related to the development of floating offshore wind power is proposed. The model is a further extension of the minimalistic prediction model for fixed-bottom wind farms previously developed by two of the authors. In the extended version, costs associated with the deployment of floating structures, such as floaters, mooring lines, and anchors, including additional installation and operational expenses, are taken into account. This paper gives an overview of the costs of the various components of different types of floating wind power installations, and using actual wind climate and bathymetry data for the North Sea, the model is employed to map the annual energy production and levelized cost of energy (LCoE) for floating wind farms located in the North Sea.

Keywords: offshore wind energy; cost modeling; levelized cost of energy; North Sea

Academic Editor: Antonio Segalini

Received: 16 December 2024
Revised: 22 January 2025
Accepted: 7 February 2025
Published: 17 February 2025

Citation: Montes, A.; Fournely, D.; Sørensen, J.N.; Larsen, G.C. Techno-Economic Modeling of Floating Wind Farms. *Energies* **2025**, *18*, 967. https://doi.org/10.3390/en18040967

1. Introduction

Wind power is one of the fastest-growing carbon neutral energy sources today. For many years, the development of wind turbines aimed at optimizing land-based wind power systems. However, due to lack of space near urban areas and increasing public resistance to large wind turbines in rural areas, most developments of wind energy systems are directed towards offshore locations today. As an illustration of this, more than 140 offshore wind farms have been erected in Europe in the past 25 years, now contributing with an installed capacity of more than 34 GW [1] and an average of approximately 3.5 GW new installations every year [2]. This development has been associated with a dramatic increase in wind turbine size, which in the past two decades has increased with a factor of 10 from about 1.5 MW in the beginning of the century to 15 MW today. Going offshore demands wind turbines to be placed on large substructures fixed to the seabed, such as monopiles and jackets, which are convenient for water depths of up to about 50 m. However, in deeper waters, fixed-bottom wind energy systems become very expensive, and for water depths of about more than 50 m, it becomes necessary to resort to floating wind turbines (FWTs), which furthermore have the potential to significantly increase the area available for offshore wind power.

Some disadvantages of offshore wind power, in general, and floating wind power, in particular, are increased costs due to expenses of substructures; the need for special support structures, e.g., in terms of special build vessels; and the added complexities associated with installation, operation, and maintenance in marine environments. According to [3], the levelized cost of energy for onshore wind power is about EUR 4 cents/kWh;

for fixed-bottom offshore wind energy, it is about EUR 8 cents/kWh; and the cost of the present floating wind power amounts to about EUR 24 cents/kWh. However, FWT technology is still in its early stage and, similar to the development of fixed-bottom offshore wind technology, driven by economies of scale and improvements in manufacturing, it is expected to undergo a steep learning curve when first taking off. Hence, according to [3], FWT technology is expected to be reduced with a factor of three, reaching a value of EUR 8 cents/kWh in 2040. To guide this development, there is a need for techno-economic models for understanding the economics of FWT farms and for providing tools to guide long-term strategic decision making.

Presently, various techno-economic models are utilized to analyze the costs of offshore wind farms, drawing on substantial experience from the operational data and expenditures of fixed-bottom wind farms as documented in published sources. Several technical reports and reviews have synthesized this information, including references such as [4–7]. Gonzalez-Rodriguez [8] provides a comprehensive overview of prominent cost models, incorporating historical data on economic factors such as inflation rates and commodity prices. Some models focus on detailed cost breakdowns of wind turbine components, such as [9], while others employ global parametrizations for parametric studies on the levelized cost of energy (LCoE) to identify key cost drivers for wind farms, for instance [10]. Additionally, international collaborative projects, like IEA Wind Task 26, have employed models combining detailed component modeling with broader industry data to establish typical LCoE values for offshore wind farms across different countries [11].

The modeling of floating wind turbines and the economic aspects of installing them are still in their infancy. Estimating the costs of floating offshore wind farms is crucial for understanding their economic feasibility. This task is challenging due to the limited number of commercial operating projects, as most are still in the research or development phase. However, breaking down the components of these floating wind farms helps assess their total cost. A major research effort is currently underway with the aim of elucidating the various costs associated with the installation, operation, and maintenance of floating wind farms. Recent investigations of the economic feasibility of floating wind farms (FWFs) have been carried out for different predefined regions, such as Portugal [12], the European part of the Atlantic Ocean [13], and the North of Spain [9]. However, these investigations generally lack details of the basic parameters characterizing the wind farm layout and wake losses, and there is a need for a simple model that takes into account the main features of FWFs to provide a fast and accurate predictive tool for assessing site-dependent energy production and costs.

This work aims to establish a straightforward, robust, and reliable numerical framework to support developers and decision makers in evaluating the economic feasibility of floating offshore wind power at a given location. The model is based on the techno-economic framework previously developed by Sørensen and Larsen [14]. Its primary objective is to facilitate preliminary cost assessments without requiring detailed technical specifications of the wind turbines or the precise layout of the wind farm. As a result, the model relies only on key inputs, such as turbine characteristics (rotor diameter and rated capacity), wind farm scale (number of turbines and total area), site-specific Weibull parameters, water depths, and distances to the coast and nearest harbor. The tool provides outputs, including average annual power generation, power density (power per unit area), capital expenditures (CAPEX), operational expenditures (OPEX), and the levelized cost of energy (LCoE).

In the following, the various aspects of the model are described. Section 2 gives an overview of the main elements of the model, including the power prediction model, a description of different platform types for FWTs, and the various components of the cost

model, including simple analytical expressions for the costs of wind turbines, transmission, floaters, mooring lines, and anchors, as well as installation costs, operational expenses, and LCoE. In Section 3, different results from the model are presented, and the LCoE is determined with the North Sea as an example. Finally, conclusions and recommendations for future work are outlined in Section 4.

2. Model and Methods

In the following, the different elements of the techno-economic model are presented. Parts of the model for fixed-bottom offshore wind farms presented in earlier works by some of the authors (see [14–16]) are exploited as the basis for the modeling. In particular, the model for determining the power production remains unchanged. The economic factors for offshore wind deployment are examined, focusing on the main cost drivers of floating offshore wind farms. They cover both CAPEX and OPEX and their impact on the LCoE. The model includes the main cost elements while keeping it simple and widely applicable. To give an overview of the model, a visual representation of the various parts of a floating wind farm is depicted in Figure 1. These parts were included in the CAPEX cost estimates, along with installation and related costs, which are later presented in detail.

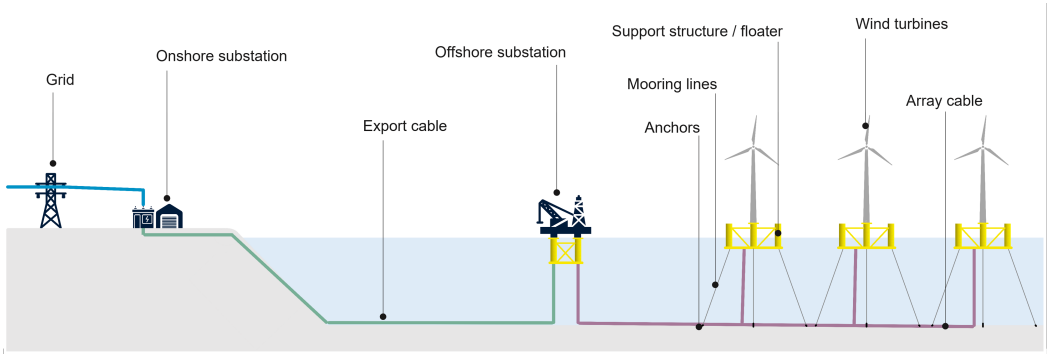

Figure 1. Schematic representation of the different elements of a floating offshore wind farm.

2.1. Power Production Model

The energy assessment model is minimalistic in the sense that only the main parameters characterizing the wind turbines and the topology of the wind farm are required (see Figure 2). In the model, the wind turbine is uniquely defined by its diameter, D, and installed power capacity, P_G. From these parameters, the rated wind speed is determined as

$$U_r = \sqrt[3]{\frac{8P_G}{\rho\pi D^2 C_{P,r}}} \tag{1}$$

where ρ is the density of air and $C_{P,r}$ is the rated power coefficient. Knowing the rated wind speed, the thrust and power coefficients are formulated as [14]

$$C_T(U) = \begin{cases} C_{T,r} & \text{for} \quad U_i \le U < U_r \\ C_{T,r}\,(U_r/U)^{3.2} & \text{for} \quad U_r \le U < U_o \end{cases} \tag{2}$$

and

$$C_P(U) = \begin{cases} C_{P,r} & \text{for} \quad U_i \le U < U_r \\ C_{P,r}\,(U_r/U)^{3} & \text{for} \quad U_r \le U < U_o \end{cases} \tag{3}$$

where U_i is the cut-in wind speed and U_o is the cut-out wind speed, and $C_{T,r}$ is the rated thrust coefficient. In most cases, thrust and power coefficients are provided by the wind turbine manufacturers. If they, for some reason, are not known, typical practical values are $C_{T,r} = 0.75$ and $C_{P,r} = 0.48$.

The wind farm topology is defined only in terms of the total number of wind turbines, N_T, and the wind farm area, A. Denoting the assumed uniform distance between the wind turbines, measured in diameters, as S, and assuming, as a simplifying approximation, that the wind farm is quadratic, the following equation gives the interspacing as a function of the wind farm area and the number of turbines:

$$S = \frac{\sqrt{A}}{D(\sqrt{N_T} - 1)} \tag{4}$$

This expression is based on the assumption that the reference wind farm has a quadratic layout (see [14]). While not all wind farms follow this configuration, it provides a straightforward approach to estimating the average spacing between turbines with reasonable accuracy, regardless of the specific layout. In practice, wind farm arrangements can vary significantly, and their exact topology is often unknown during the early planning stages.

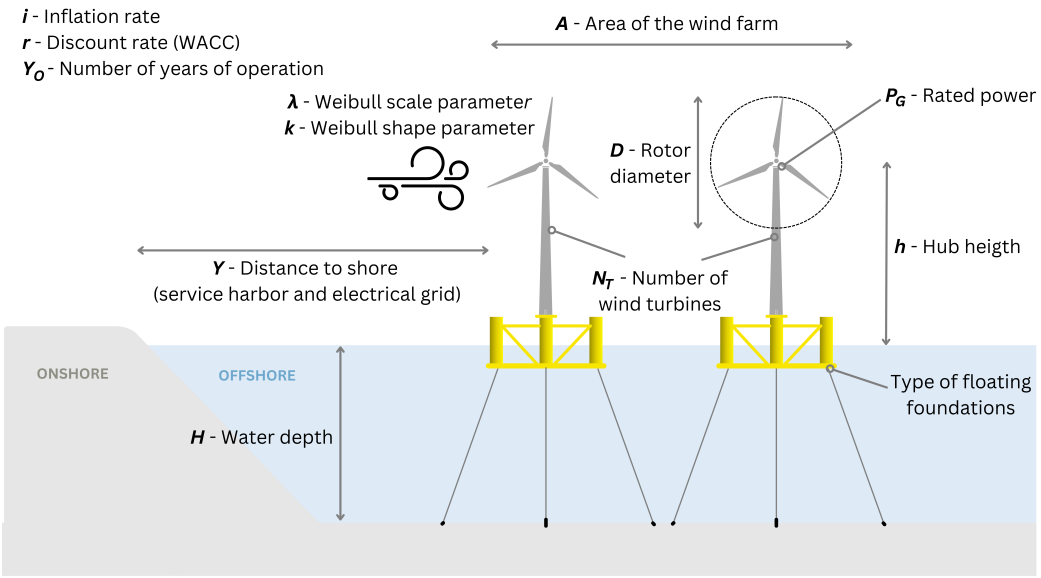

Figure 2. Scheme of the input parameters to the minimalistic model, allowing calculation for energy production, CAPEX, OPEX, and LCoE.

The power production model is based on the atmospheric wind farm boundary layer model developed by Frandsen [17], which evaluates wake effects and their interaction with the atmospheric boundary layer. This model assumes that the wind farm is sufficiently large for the wind field within it to reach equilibrium with the surrounding atmospheric boundary layer (ABL) flow. As a result, the model derives the following simplified equation to estimate the wake-affected mean wind speed at hub height within the wind farm:

$$U_h = \frac{G}{1 + ln\left(\frac{G}{f'h}\right)\frac{\sqrt{c_t + (\kappa/ln(h/z_o))^2}}{\kappa}} \tag{5}$$

where $\kappa = 0.4$ is the von Kàrmàn constant; G is the geostrophic wind speed; $f' = f \cdot \exp(A*)$, with $f = 2\Omega\sin(\phi)$ being the Coriolis parameter with Ω denoting the rotational speed of the globe; ϕ is the latitude; and $A*$ is a constant, which is approximately equal to 4 at latitude $\phi = 55°$. For more information, we refer to a paper by Frandsen et al. [18], where the method is described in more detail. The essential parameter in the above expression is $c_t = \frac{\pi C_T}{8S^2}$, which is the parameter that determines the impact of the turbine thrust on the boundary layer profile.

To estimate wind farm power production and provide inputs for the cost model related to operations and maintenance (O&M) expenses, it is necessary to determine the mean wind speed statistics both for the undisturbed site (ambient wind speed statistics) and within the wind farm flow field. A two-parameter Weibull distribution, $\Phi = \Phi(\lambda, k)$, where λ represents the scale parameter and k the shape parameter, is used to characterize the annual wind speed distribution. However, the wind speed statistics inside a wind farm differ from those of the ambient flow due to wake-induced reductions caused by neighboring turbines. To estimate the annual power production of a turbine within the wind farm, the Weibull scale parameter is adjusted to reflect the wind conditions at hub height for turbines operating within the array.

Since the model described above assumes a fully developed atmospheric boundary layer in equilibrium with an infinitely large wind farm, a correction is required to account for the finite size of actual wind farms. To approximate this effect, the following simple heuristic expression is applied to adjust the wind farm power production estimate:

$$P_E = (N_T - a\sqrt{N_T})P_{WF} + a\sqrt{N_T})P_{Free} \quad (6)$$

where P_E represents the average total annual power production, P_{WF} denotes the average power output of a single wind turbine affected by wake losses, P_{Free} corresponds to the average production of an isolated wind turbine operating in free-stream conditions, and a is a correction factor. This expression is based on the assumption that the correction depends on the proportion of turbines located along the wind farm's edges relative to the total number of turbines. Given that wind turbines can be arranged in various configurations, a general approach considers a square-shaped wind farm with $\sqrt{N_T}$ turbines along each edge, leading to a total of $4\sqrt{N_T}$ edge turbines. Since the turbines positioned along two of these edges are exposed to the free-stream wind, the power output from approximately $2\sqrt{N_T}$ turbines is expected to be equal to that of standalone turbines. Additionally, depending on the wind direction, some turbines near the farm's perimeter may also experience reduced wake effects. Consequently, while some turbines operate under fully developed wake conditions, others are only partially affected, and those on the upwind-facing edges remain unaffected by wakes. In this work, a correction factor of $a = 3$ is applied, indicating that, on average, 3/4 of the turbines along the wind farm's perimeter experience free-stream conditions. This assumption has demonstrated good agreement when comparing estimated wind farm production with actual recorded data [14]. However, ongoing research is examining the impact of additional parameters, such as turbine spacing and wind speed, on the value of a.

A detailed explanation of the model, along with the derivations of its equations, can be found in a study by Sørensen and Larsen [14], where it is thoroughly described and validated against actual performance and cost data from several full-scale wind farms. The accuracy of the predicted annual energy production is shown to be within approximately 5%. Despite its simplicity, the model demonstrates a remarkable ability to estimate both costs and power output for offshore wind farms with high reliability.

2.2. Categorization of Floating Wind Turbine Types

The following subsection gives an overview of different types of floating wind turbines. The different concepts imply different costs, and it is therefore required to distinguish them in the following cost assessment.

2.2.1. Floating Platforms

A key difference between floating and fixed-bottom offshore wind installations is the design of the platform. Traditional offshore wind turbines use monopile or jacket

foundations, which limit their use to waters with about less than 50 m depth. Floating offshore wind can access wind resources in deeper, more stable waters, offering significant growth potential for the offshore wind sector.

Floaters are usually classified on the basis of their primary stabilization methods. There are three main ways to ensure the stability of a floating system: ballast, buoyancy, and mooring. The main types of floating support structures are semi-submersible/barge, spar, and tension leg platform, as shown in Figure 3. In general terms, semi-submersibles are mainly stabilized by buoyancy, spars are stabilized by ballast, and tension leg platforms are stabilized by mooring tension. To provide a better understanding of these technologies, a brief description of each is provided.

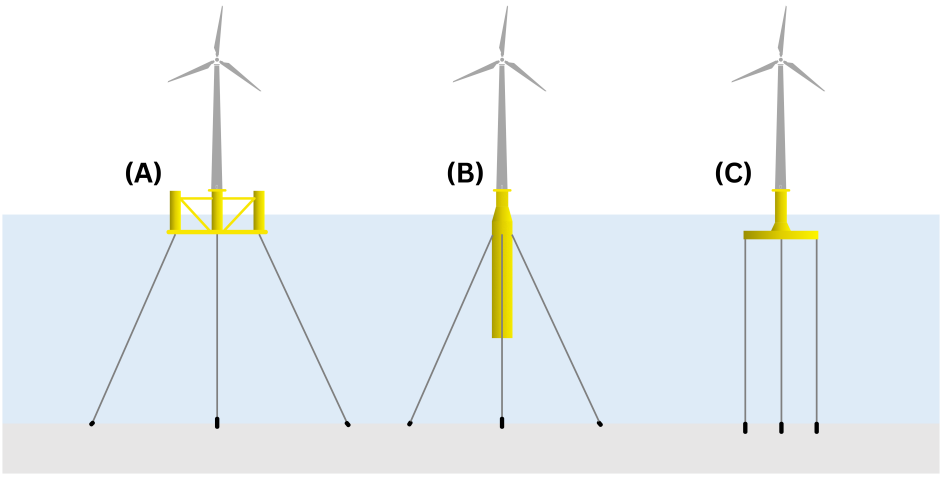

Figure 3. Types of floating wind turbine platforms: (**A**) semi-submersible, (**B**) spar, and (**C**) tension leg platforms.

- **Semi-submersible/barge (SSP):** Semi-submersibles and barges are two key types of floaters that use water-plane stabilization. Semi-submersibles achieve stability with several smaller separate water-plane areas, usually with three columns arranged in a triangle for optimal stability. Sometimes, a fourth column is added in the center to support the wind turbine. This design allows for onshore construction and towing to the site, avoiding the need for expensive construction vessels with marine cranes. Its shallow draft allows it to be used in waters as shallow as 40 m. The platform can be detached from its moorings for maintenance, making maintenance easier. Barges use a similar stabilization method but have a single large central water-plane area instead of multiple cylinders.
- **Spar buoy (SB):** Spar buoys use ballast for stability and are usually shaped like long cylinders similar to a ship's hull. They have a deep draft, providing ample room for wind turbines and equipment, and are anchored to the seabed with mooring lines. The foundation is a steel or concrete cylinder filled with water and gravel ballast to stay stable. Spar buoys need deeper water, usually starting at 80 m.
- **Tension leg platforms (TLP):** TLPs use mooring for stability and support the wind turbine with a central cylindrical structure connected to three or more outward-extending pontoons. Vertical tendons, anchored by suction piles, driven piles, or template foundations, provide pre-tensioned stability to keep the platform upright. This technology is suitable for water depths of 50–60 m or more. TLPs can be assembled onshore, avoiding the logistical challenges of offshore assembly.

The motion of the floating support structure is largely governed by the mooring system, which varies among the three primary floater types: spars and semi-submersibles/barges use catenary or taut mooring lines, while TLPs are anchored with tendons. For floaters

employing chains or ropes in a catenary configuration, the wave frequency range exceeds the natural frequencies in all six primary motion directions. In contrast, for tendon-moored floaters, this applies only to the natural surge, sway, and yaw frequencies.

In summary, Table 1 offers a comparative overview of the primary characteristics, advantages, and limitations of semi-submersibles, TLPs, and spar buoys, providing valuable context for understanding their deployment and operational trade-offs. The development of floating offshore wind turbines has expanded the potential to harness wind energy in deeper waters, with spar buoys, semi-submersibles, and tension leg platforms being the three primary types of floater utilized for wind turbines, each with a unique approach to ensure stability. The dynamics of these floaters depend on how they are anchored.

Table 1. Comparison of different types of floaters based on [19].

Type	Strengths	Weaknesses
Semi-submersible	- Shallow water suitable - Simple assembly - Broad installation window	- High motions - Large footprint - Complex structure - Susceptible to corrosion - Heavy, costly structure - Long mooring lines
TLP	- Intermediate depth suitable - Low motions - Small footprint - Little corrosion - Shorter mooring lines	- Unsuitable for shallow waters - High risk if mooring fails - Complex installation - High structural stress
Spar	- Simple structure - Low corrosion - High sea state suitability	- Unsuitable for shallow water - Challenging assembly - Large footprint - High installation costs

2.2.2. Mooring Lines and Anchors

Within the floating wind industry, three primary mooring configurations draw inspiration from the oil and gas sector. These configurations, adapted for floating wind farms, include catenary, tension leg, and taut or semi-taut systems, illustrated in Figure 4. Each is briefly described in the following:

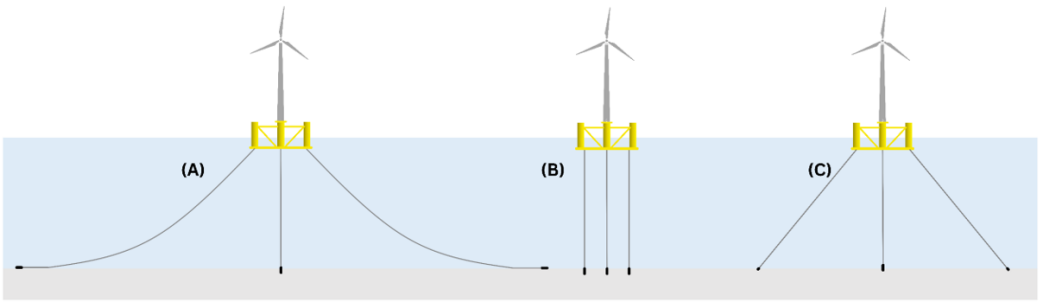

Figure 4. Three types of mooring systems: (**A**) catenary mooring system, (**B**) tension leg mooring system, and (**C**) taut or semi-taut mooring system.

- Catenary mooring systems employ freely hanging steel chains between the floating structure and the anchor, forming a catenary shape. This design allows the floating platform freedom of vertical and horizontal movements, enhancing flexibility. Catenary systems are known for their cost-effectiveness and adaptability to various water depths and weather conditions. However, they face limitations regarding the

maximum length of the mooring line and susceptibility to lateral forces, making them most suitable for shallower waters and moderate environmental conditions.

- Tension leg mooring systems utilize pre-tensioned mooring lines, allowing the floating body to achieve full tension. These systems are more suitable for deep-water applications, providing high stiffness and stability for improved motion control of the floating structure. Pre-tensioned tendons aid in reducing vertical motions and establishing a rigid connection to the seabed.
- Taut or semi-taut mooring systems maintain tension in the mooring lines, unlike catenary systems, which allow slack to form in a catenary curve. This design strikes a balance between the flexibility of catenary systems and the stiffness of tension leg systems. Taut or semi-taut systems are preferred in deeper waters and more challenging environmental conditions, where a combination of flexibility and stiffness is desired.

Selecting the right mooring system for a floating wind turbine involves considering factors such as the type of floater, water depth, seabed conditions, and costs. Therefore, it is crucial to thoroughly assess these factors to choose the most suitable mooring system for a project.

When discussing mooring lines for floating offshore wind farms, the choice of material is also important. Common materials include studless chains, known for their cost effectiveness and easy handling in permanent mooring systems, and synthetic ropes like polyester and HMPE, which offer different levels of flexibility and stiffness to suit various conditions [4]. The number of mooring lines is another key factor in mooring system design. While most mooring setups use three lines or clusters, certain floater designs, like those with four corner buoyancy columns, may need four-line systems. Although redundant multi-line clusters are not common, future developments driven by operational experience may trend towards more redundant systems [4].

Regarding anchors, there are various types, including drag embedment anchors (DEAs), vertical load anchors (VLAs), and suction piles [20,21], depicted in Figure 5.

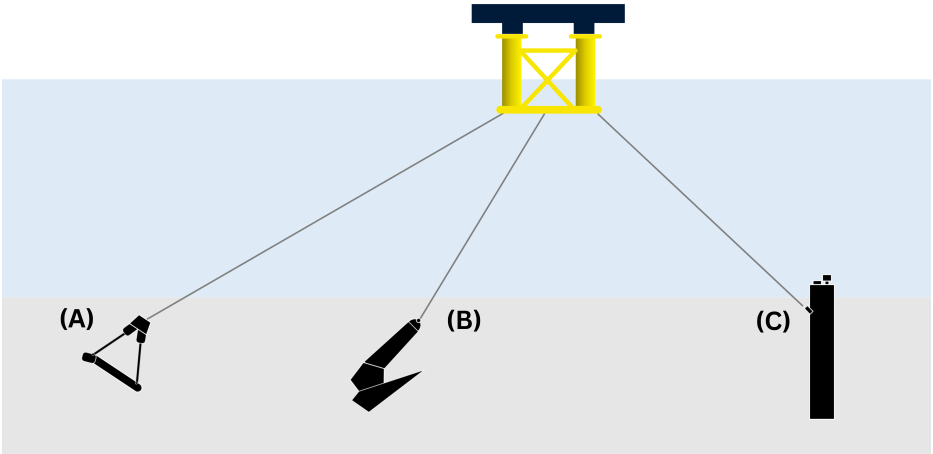

Figure 5. Types of anchors for floating wind turbine platforms: (**A**) vertical load anchor, (**B**) drag embedment anchor, and (**C**) suction pile anchor.

Their capabilities are summarized as follows:

- **VLA (vertical load anchor):** VLAs are suitable for taut leg mooring systems, deployed in water depths exceeding 400 m. Designed to withstand vertical loads, VLAs rely on their weight to provide stability, suitable for various seabed conditions and particularly effective in shallower water depths.

- **Drag embedment:** This anchoring technology involves horizontally dragging the anchor into the seabed, gaining popularity for shallow water applications. Drag embedment anchors (DEAs) rely on their weight and shape to resist horizontal forces from wind, waves, and currents, effectively working in different seabed conditions.
- **Suction pile:** Suction piles excel in deep-water applications, handling both horizontal and vertical loads. These large steel or concrete structures create a firm grip on the seabed through suction, stabilizing the floating platform, particularly effective in softer seabed conditions like clay and fine sand.

2.3. Cost Modeling

Following the benchmark made on existing technologies, the cost of each part of a floating turbine is assessed. To build up a general cost model, the aim is to derive cost estimates that only depend on a set of parameters that developers would use to describe a project in early-stage development. This list of relevant input parameters is given in Table 2. Each component of the floating wind farm is analyzed based on these parameters. Key input drivers are identified from the list, and straightforward relationships between cost and these inputs are established.

Table 2. Main input parameters affecting costs.

Name	Symbol	Value	Units
Rated power	P_G	Variable	MW
Rotor diameter	D	Variable	m
Number of turbines	N_T	Variable	-
Water depth	H	Variable	m
Hub height	h	Variable	m
Wind farm area	A	Variable	m^2
Distance to shore	Y	Variable	km
Number of years of operation	Y_O	Variable	-
Wind farm density	d_{WF}	Variable	MW/km^2
Rated power coefficient	$C_{P,r}$	0.48	-
Rated thrust coefficient	$C_{T,r}$	0.75	-
Air density	ρ	1.225	kg/m^3
Gravitational acceleration	g	9.816	m/s^2

For the purposes of this model, the rated power of the wind turbines, P_G, is considered to range from 5 to 15 MW. This range reflects the current market availability of commercial wind turbines, as well as the typical power ratings for prototypes designed for floating foundations that we have used to develop this model. The water depth, denoted as H, is assumed to vary between 40 m and 1000 m. A lower limit of 40 m is selected because it is the minimum depth for which semi-submersible foundations are considered viable, while an upper limit of 1000 m represents the maximum theoretical water depth for floating wind farms. The distance to shore, denoted as Y, is constrained between 5 and 200 km. This range is chosen because distances beyond 200 km make the installation and maintenance of the wind farm unfeasible due to increased logistical challenges and costs.

2.3.1. Wind Turbine

Wind turbine costs are mainly influenced by the rated power. Floating turbines are generally more costly than bottom-fixed ones, as they require stronger and heavier towers to keep natural frequencies outside the wave excitation range [22]. Accurately assessing this additional weight and its impact on costs is challenging due to limited data. Floating turbines are often approximated as equivalent to bottom-fixed ones, which can introduce

errors in cost estimation. Future research aims to refine cost predictions as more data become available.

To evaluate the current wind turbine costs and determine if there have been changes from a previous model [14], several data sources have been reviewed, as summarized in Table 3. The comparison presented in Table 3 includes cost data from various years and sources, adjusted to 2022 values for consistency. These adjustments were made using inflation rates obtained from [23], ensuring that all cost models are normalized to a common baseline. This approach allows for a fair comparison of values across different years and sources.

Table 3. Comprehensive breakdown of cost sources for offshore wind turbine prices.

Data Source	Year	Cost Model [M€]	Cost Model [M€$_{2022}$]
[8]	2017	$1.347 \cdot P_G^{0.87}$	$1.560 \cdot P_G^{0.87}$
[10]	2019	$1.700 \cdot P_G$	$2.113 \cdot P_G$
[11]	2021	$1.374 \cdot P_G^{0.87}$	$1.594 \cdot P_G^{0.87}$
[24]	2020	$-1.900 + 1.600 \cdot P_G$	$-2.109 + 1.776 \cdot P_G$
[25]	2019	$1.128 \cdot P_G$	$1.271 \cdot P_G$
[26]	2021	$1.220 \cdot P_G$	$1.348 \cdot P_G$
[27]	2022	$1.290 \cdot P_G$	$1.290 \cdot P_G$
[28]	2022	$1.440 \cdot P_G$	$1.440 \cdot P_G$

The analysis suggests that costs have remained relatively stable. Consequently, the following Equation (7), which was previously employed in [14], is still valid for estimating wind turbine costs.

$$C_{WT} = N_T \cdot 1.25 \cdot (-0.15 + 0.92 \cdot P_G) \tag{7}$$

where P_G is measured in MW and C_{WT} is given in M€.

2.3.2. Transmission System

Numerous factors shape the cost structure of the offshore wind energy transmission system, which has an impact on both financial and technical aspects. Key cost drivers include the following:

- **Inter-turbine distance (array cables):** The distance between turbines within the wind farm determines the length of array cables needed. Larger distances require longer cables, increasing both material and installation costs.
- **Proximity to onshore grid connection (export cable):** The distance from the offshore wind farm to the onshore grid connection affects the length of the export cable. Longer distances require more cables, raising the costs of material, installation, and burial. In this analysis, this distance is referred to as the distance to the shore, labeled as Y.
- **Aggregate power capacity of wind farm (offshore substation):** The total power output of the wind farm impacts the design and capacity of the offshore substation. Higher power output necessitates larger substations, increasing infrastructure and equipment costs.

The above factors are interconnected and determine the overall costs of the transmission system in floating offshore wind farms. Their impact is highlighted in three major studies evaluating transmission system costs that result in the equations shown in Table 4. Among these sources, only one study [10] accounts for the costs of the onshore substation.

Therefore, these costs are excluded from our analysis and approximated as 9% of the total capital expenditure based on previous models [14].

Table 4. Comprehensive breakdown of cost sources for offshore transmission system prices.

Data Source	Year	Cost Model [M€$_{2022}$]
[8]	2017	$0.359 \cdot L_I + 0.748 \cdot Y + 0.539 \cdot (N_T \cdot P_G)^{0.861}$
[10]	2019	$0.323250 \cdot L_I + 0.5096 \cdot Y + 0.36907 \cdot N_T \cdot P_G$
[29]	2018	$0.0390 \cdot L_I + 0.0629 \cdot e^{(234.34 \cdot P_G \cdot N_T / (105 \cdot 36000))} + 0.2 \cdot Y + 2.21 + 0.076 \cdot P_G \cdot N_T$

The total cost of the transmission system is calculated using equations that average the estimates of previous models, encompassing array cables, export cables, and the offshore substation. These equations, expressed in M€, provide a robust framework for estimating transmission system expenses in floating offshore wind farms. The expressions for C_{ac}, C_{ec}, and C_{off-s} were derived by averaging the cost components across the three studies presented in Table 4. Adjustments were made to align with the methodologies and weightings of the referenced models. For instance, C_{ac} reflects a weighted average of L_I-related coefficients and incorporates terms for exponential scaling from [29]. C_{ec} averages the coefficients for Y, while C_{off-s} combines the scaling terms for $P_G \cdot N_T$ from the three studies. These equations provide an aggregated approximation of costs that balances assumptions from different methodologies.

$$C_{TS} = C_{ac} + C_{ec} + C_{off-s} \tag{8}$$

$$C_{ac} = 0.275 \cdot L_I + 1/3 \cdot 0.055 \cdot e^{234.34 \cdot P_G \cdot N_T / (36000 \cdot 10^5)} \tag{9}$$

$$C_{ec} = 0.556 \cdot Y \tag{10}$$

$$C_{off-s} = 0.168 \cdot P_G \cdot N_T + 1/3 \cdot (2.53 + 0.625 \cdot (P_G \cdot N_T)^{0.861}) \tag{11}$$

where

$$L_I = S \cdot D \cdot (N_T - 1)/1000 \tag{12}$$

2.3.3. Floater

Floating platforms are typically designed considering factors such as buoyancy, stability, motion response, and structural integrity. Due to the unique requirements of wind turbines and wave conditions, a simplified model is necessary. The cost model aims to link platform size to the turbine's rated power through the following three-step process:

1. Establish a relationship between rated power and platform weight based on a sample of tested prototype floaters.
2. Determine material composition and mass breakdown.
3. Calculate material costs multiplied by weight.

To perform step 1, data on existing prototypes, including six semi-submersible platforms and five spar platforms, have been gathered. To estimate the platform's total mass as a function of the wind turbine's rated power, the following two methods are outlined in [22]:

- Regression-based scaling laws: Two fitting methods are proposed. The first assumes a power-law relationship $y = c \cdot x^b$, where x is the rated power, y is the platform's total mass, and c and b are unknown coefficients. The second uses a heuristic approach with $y = c \cdot x^d + f$, where c, d, and f are unknown.

- Scaling from a reference platform: Mass is estimated by scaling a reference platform based on turbine and platform dimensions. For turbines, the scaling factor is $s = D_{scaled}/D_{base}$ (rotor diameter), and for platforms, $p = L_{scaled}/L_{base}$ (e.g., draft). Using these factors, the following two scaling laws are applied:
  - Power scaling law: $p^3 = s^3$, giving

$$m_{scaled} = m_{ref} \cdot \left(\frac{P_{scaled}}{P_{ref}} \right)^{3/2} \tag{13}$$

  - Mass scaling law: $p^3 = s^2$, giving

$$m_{scaled} = m_{ref} \cdot \left(\frac{P_{scaled}}{P_{ref}} \right) \tag{14}$$

At this stage, several equation possibilities were considered to establish a relationship between the platform's total mass and the wind turbine's rated power for both spar and semi-submersible types. For spar platforms, the consistent data from the design prototypes allowed the derivation of the optimal regression coefficient using a heuristic approach (Equation (16)). In contrast, the wide variation in semi-submersible designs made robust regression challenging. A mass scaling law expression was therefore selected to best represent the relationship between total mass and rated power for semi-submersibles based on a central data prototype point (Equation (15)).

$$m_{total} = 1946 \cdot P_G \tag{15}$$

$$m_{total} = 2 \cdot P_G^{3.45} + 6796 \tag{16}$$

To perform steps 2 and 3, it has been noticed that these prototypes have been designed for various wind turbine capacities and vary in design complexity and materials, which affects their costs. For example, semi-submersible platforms predominantly use steel and water for ballast, while spar platforms use concrete. The cost analysis also considers manufacturing expenses, accounting for platform shape complexity and the type of ballast used. Moreover, based on the same prototypes, it has been considered that 26% of the total mass of semi-submersible platforms is steel, valued at a cost of EUR 903/tonne [30], while for spar platforms, 18% of the mass consists of steel, with the remaining 82% being concrete, priced at EUR 81.3/tonne [31].

2.3.4. Mooring Lines

The CAPEX of the mooring lines is determined by multiplying the total length of the lines by the cost of the material. In mooring lines studies, load scenarios and safety margins are considered to assess the length, composition, and number of mooring lines. Taut/semi-taut and catenary lines are suitable for both spar and semi-submersible floating platforms, but the taut/semi-taut design criteria are more complex and depend on specific environmental conditions. Then, the cost calculation has only been made assuming catenary lines for the mooring line cost estimation. Using classical mechanics principles [32], it is possible to show that the length of the mooring line, l, depends on the maximum horizontal tension applied in the fairlead position, T_{max}, and the integration of the gravity and buoyancy forces acting on each chain element, wH. w corresponds to the average mass of a unit length of a studless chain mooring line considered underwater (i.e., including the buoyancy effect), multiplied by the gravitational pull of the Earth, $g = 9.8$ m/s^2. In short, $w = (m_{ML} - \rho_{\text{water}} A_s)g$, where m_{ML} is the chain's mass per unit of length, ranging around $m_{ML} = 689$ kg/m, and A_s is the mooring line section area considering a diameter

of the chain of 200 mm as referenced in [4,33]. The assumption of a constant chain section simplifies the cost analysis, as the impact of variations in chain section dimensions is partially offset by adjustments in mooring line lengths in a more complex optimization problem. This approach appears as a reasonable choice for an initial estimation and also aligns with industry standards, which often define chain dimensions within specific ranges based on water depths and load conditions. The density of steel is assumed to be $\rho_{\text{steel}} = 7750\ \text{kg/m}^3$. H corresponds to the water depth at the wind turbine position.

$$l = H\sqrt{\frac{2T_{max}}{wH} - 1} \tag{17}$$

This result is obtained by neglecting the bending stiffness, dynamic effects, and hydrodynamic forces. The maximum load on the position of the fairlead, T_{max}, is assessed considering the forces of wind, wave, and current, assuming that all these forces are applied in the same direction and parallel to the mooring line studied, corresponding to a worse-case scenario. In order to obtain a general expression of the maximum load in the fairlead position, this load is assessed as a function of the wind thrust force alone $F_{T,max}$. Using the wind turbine and the floater described in [34], the wave force, current force, and wind thrust force are evaluated, showing that the total force is 2.2 times higher than the thrust force alone. In addition to the horizontal force acting in line with the mooring line, it must also endure tension from the weight of the two opposing mooring lines. For a scenario with three mooring lines spaced at 120° angles, the tension from the opposing mooring lines equals $wH\cos(60^\circ) + wH\cos(60^\circ) = wH$. Therefore, the maximum load can be expressed as

$$T_{max} = 2.2 \cdot F_{T,max} + wH \tag{18}$$

Thus, the length of one mooring line is described as

$$l = H\sqrt{\frac{2 \cdot (2.2 \cdot F_{T,max})}{wH} + 1} \tag{19}$$

This cost estimation focuses on steel chains, even if synthetic ropes might replace them in challenging locations. The cost per unit of mass in air of the steel chain is obtained by calculating the average of several sources [33,35–37], which resulted in $c_{ML} = 2.868\ €/\text{kg}$.

The number of mooring lines is set to 3, a typical value to guarantee stability, although subject to cost-risk analysis. Therefore, the total cost of the anchor lines is calculated using the number of wind turbines N_T, the number of mooring lines N_{ML}, the chain cost c_{ML} per unit of mass m_{ML}, and the length of a single mooring line l, as follows:

$$C_{ML} = N_T \cdot N_{ML} \cdot c_{ML} \cdot l \cdot m_{ML} \tag{20}$$

2.3.5. Anchors

The cost analysis for anchors in floating offshore wind turbine support structures is based on one study [38], which reviews three common anchor technologies used in offshore wind projects: drag embedment, vertical load anchor (VLA), and suction piles. The study provides a comparative cost analysis of each technology, covering both anchor and installation expenses. Additional information on installation costs is given in Section 2.3.6. Table 5 offers a detailed cost breakdown in M€ for each technology. In this table, T_{anchor} represents the line tension at the anchor point, measured in kN. This tension is calculated using Equation (21) for the maximum load scenario, where $T_{max} = 2.2 \cdot F_{T,\text{max}} + wH$, and considering the mooring line section area A_s.

$$T_{anchor} = 2.2 \cdot F_{T,max} + wH - \rho g A_s H \tag{21}$$

Another study [21] suggests that the choice of anchor technology depends on water depth. In shallow waters, drag embedment anchors are preferred, whereas VLA anchors are suitable for depths exceeding 400 m, especially in taut leg mooring systems. Suction pile anchors, capable of handling both horizontal and vertical loads, are commonly used in tension leg mooring lines and sometimes in taut leg systems in deeper waters. This classification guides the model's implementation. However, it is essential to note that these are rough estimates. The selection of an anchor type should involve a soil test and a thorough tension analysis to ensure optimal performance. With proper selection and application of these anchor technologies, effective mooring of floating offshore wind turbines is achievable at various water depths.

Table 5. Anchor costs obtained from [38].

Anchor Technology	M€ [Line Tension]
Drag embedment	$108 \cdot T_{anchor} \cdot N_{anchors} \cdot 10^{-6}$
VLA	$129 \cdot T_{anchor} \cdot N_{anchors} \cdot 10^{-6}$
Suction pile	$162 \cdot T_{anchor} \cdot N_{anchors} \cdot 10^{-6}$

2.3.6. Installation

This section explains how the installation of floating wind farms differs from that of traditional fixed-bottom offshore wind farms, and describes the most important steps and costs involved in the installation.

Wind turbine installation: Floating wind turbines are usually assembled either onshore or in protected areas close to the port. This process involves putting together different parts, such as the tower, nacelle, rotor blades, and electrical systems. Onshore assembly is often chosen because it reduces the risks associated with lifting operations at sea and possible delays caused by bad weather. It is important to mention that the installation costs of wind turbines are included in the overall costs of the floating platform.

Floating platforms installation: The installation techniques for floating platforms differ depending on the type of substructure chosen, which significantly affects the installation costs. Various installation scenarios are considered, taking into account factors like the space available in shipyards, draft, the number of liftings, and logistics for transportation. Among these scenarios, the following two are particularly notable:

- For spar platforms, an onshore installation method is employed, followed by wet transport of the offshore wind generator and the floating structure. This approach requires an onshore crane and a tug.
- In contrast, semi-submersible platforms use dry transport of the offshore wind turbine and the floating structure on a barge, with a floating crane (without storage) for their offshore installation.

The installation cost per MW and wind turbine is expressed in M€ [9].

$$C_{i,\,WT-spar} = 0.2157 \cdot N_T \cdot P_G \tag{22}$$

$$C_{i,\,WT-semisub} = 0.2067 \cdot N_T \cdot P_G \tag{23}$$

Transmission system installation: Installation costs for the transmission system are determined using methodologies and sources similar to those for the transmission system components. The average costs from various references [8,10,29] are combined to calculate the installation cost of the transmission system, covering array cables, export cables, and offshore substations, expressed in M€.

$$C_{i,\,TS} = 0.146 \cdot L_I + 0.128 \cdot Y + 0.015 \cdot N_T \cdot P_G \tag{24}$$

Mooring lines installation: The installation expenses associated with mooring lines are derived from pertinent literature [13]. The installation cost equation is as follows, in M€:

$$C_{i,\,ML} = 0.2533 \cdot N_T \tag{25}$$

Anchor costs: The installation costs for mooring lines are obtained from the same source as the anchor costs [38]. The equation for calculating installation costs is provided in Table 6.

Table 6. Anchor installation costs obtained from [38].

Anchor Technology	M€ [Installation]
Drag embedment	$4644 \cdot N_{anchors} \cdot 10^{-6}$
VLA	$7430 \cdot N_{anchors} \cdot 10^{-6}$
Suction pile	$10{,}217 \cdot N_{anchors} \cdot 10^{-6}$

It is important to note that the methodologies and cost estimates may vary depending on the sources referenced. These insights help to provide a comprehensive understanding of the installation costs related to floating offshore wind farms.

2.3.7. Operational Expenses

Operational expenses represent a significant element in the financial planning and long-term sustainability of wind farms. Several studies have proposed methodologies for estimating O&M costs. In particular, a study [13] introduces a cost model that incorporates a base cost that is dependent on the capacity of the wind farm in megawatts (MW) and includes an additional component for travel expenses, which are influenced by the distance to shore. However, given the relatively limited number of large-scale floating offshore wind farms, there is a lack of empirical cost data, which complicates the precise estimation of O&M expenses. More research on failure rates and the resources required for repairs and maintenance will be critical to reducing O&M costs. As the literature indicates, various strategies are being explored, but additional research is necessary to identify the most effective approach for O&M in offshore wind farms.

In light of this, further work has been conducted to refine the equation proposed in a previous study [39]. This updated model is based on data from Danish, British, and German wind farms, making it more grounded in real-world observations. As such, despite it not being tailored to floating wind farms, this equation has been adopted, which is expressed in M€ as

$$C_{O\&M} = P_G \cdot N_T \cdot 7.224 \times 10^{-2} \cdot C_f^{0.84} \cdot Y^{0.19} \cdot d_{WF}^{0.22} \tag{26}$$

where C_f is the capacity factor of the wind farm (the expected annual energy produced divided by its theoretical maximum), and d_{WF} is the power density of the wind farm (the rated power divided by the total area).

2.4. Levelized Cost of Energy

The levelized cost of energy is used to compare technology costs and assess economic viability over time. Combining cost and energy production into a single metric determines the minimum selling price of energy needed for project profitability. To compute LCoE, the following expression is used:

$$LCoE = \frac{\sum_{t=0}^{n} \frac{I_t + M_t}{(1+r)^t}}{\sum_{t=0}^{n} \frac{E_t}{(1+r)^t}} \tag{27}$$

where E_t is the energy production in year t, I_t is the investment in year t, M_t is the operation and maintenance expenditure in year t, n is the project lifespan, and r is the discount rate, typically the Weighted Average Cost of Capital (WACC). WACC is a measure of the average cost of financing a project, considering both equity and debt contributions. It is calculated as

$$WACC = E_{\%} \cdot i_e + D_{\%} \cdot i_d \tag{28}$$

where

$$E_{\%} = \text{the percentage of the project financed by equity (20–35\%);} \tag{29}$$
$$i_e = \text{the return rate expected by equity investors;} \tag{30}$$
$$D_{\%} = \text{the percentage of the project financed by debt (65–80\%);} \tag{31}$$
$$i_d = \text{the interest rate paid on the debt.} \tag{32}$$

In simple terms, WACC represents the weighted cost of money the project uses, combining what is paid to lenders (interest on debt) and what is required by investors (returns on equity).

Supported by the Danish Energy Agency [40], 5% WACC is used, acknowledging that while floating projects have higher risks, technological advancements can reduce costs, aligning their WACC with bottom-fixed projects over time.

Inflation, averaged at 2.2% from the World Bank data [23], is crucial for estimating increases in OPEX during the project's lifetime. With CAPEX being accounted for in year 0 and OPEX calculated from year 1, the equation for LCoE adjusted for inflation is given as

$$LCoE = \frac{\sum_{t=0}^{Y_O} \frac{CAPEX + OPEX_t \cdot (1+i)}{(1+r)^t}}{\sum_{t=0}^{Y_O} \frac{E_t}{(1+r)^t}} \tag{33}$$

where i is the average inflation rate, assumed to be 2.2% based on World Bank data, and Y_O is the project's operational years.

3. Results and Discussion

In the following, different results computed by the developed model will be presented and discussed. The basics of the model have, in earlier works, been validated against available data for existing bottom-fixed wind farms. Furthermore, as mentioned in the introduction, driven by the economics of scale and improvements in manufacturing, the actual costs of FWFs are expected to decrease dramatically in the years to come. Hence, an FWF cost model is not static and needs to be updated continuously. However, the present cost model can be utilized to demonstrate the expected added expenses to fixed-bottom WFs and to compare the relative costs of the various components of FWF power systems.

3.1. Comparative Study of Costs

A detailed case study has been carried out to examine the costs calculated from the model using input parameters that represent typical values for an offshore wind farm. As a reference case is chosen a wind farm consisting of 100 15 MW wind turbines located 9 rotor diameters from each other at a water depth of 150 m and a distance of 50 km to the shore (see Table 7). The parameter Y_O represents the number of years of operation of the wind farm, which in this case is assumed to be 20 years. Based on this, a separate parametric study is performed for analyzing the expenditures as function of the distance to the shore and the water depth. The reason for choosing a 15 MW wind turbine as a reference is to mirror current marked trends in turbine size to ensure that the analysis aligns with current industry standards.

Table 7. Input parameters for a floating offshore wind farm case.

Parameter	Cost Analysis (Figure 6)	Cost Analysis (Figure 7a)	Cost Analysis (Figure 7b)
A	394 km^2	394 km^2	394 km^2
N_T	100	100	100
P_G	15 MW	15 MW	15 MW
D	245 m	245 m	245 m
h	150 m	150 m	150 m
H	150 m	Variable	150 m
T	Semi-submersible	Semi-submersible	Semi-submersible
Y	50 km	50 km	Variable
i	2.2%	2.2%	2.2%
r	5%	5%	5%
Y_O	20 years	20 years	20 years

The expenditures for the various cost components for the full lifetime of the floating wind farm is shown in Table 8, where the columns represent costs [M€], costs per installed power capacity [M€/MW], and percentage of the total costs. It is seen here that, altogether, OPEX and the costs of the platform and the wind turbine constitute about 2/3 of all expenses, with OPEX constituting the biggest share at 26.2%, followed by the platform with 21.3% and the wind turbine with 19.5%. Unfortunately, OPEX is also the most uncertain expense as knowledge about operation and maintenance of FWTs is still very limited. In the present work, the model used to represent OPEX is taken from fixed-bottom experiences; hence, it represents an ideal case corresponding to what can be expected when the floating technology has matured to the same technological level as the one of fixed-bottom wind plants. According to Centeno-Telleria et al. [41], OPEX constitutes about 25% of the total expenditure for the present bottom-fixed wind farms in the North Sea and about 43% for the present pilot floating wind farm projects. The latest value is not necessarily a good reference as it corresponds to prototype floating projects, and the current planned projects are of a different size. Ref. [41] estimates a value of about 21% as an ideal long-term goal for floating projects, which better align with the 26.2% obtained in this study case.

The pie diagram in Figure 6 displays the proportional breakdown of CAPEX. Similar to fixed-bottom wind farms, wind turbine costs make up one of the largest shares, nearly 27% of the total costs. However, in floating wind farms, platform costs, analogous to foundations in bottom-fixed setups, are of the same order of magnitude, accounting for about 29% of the total costs. Thus, wind turbines and platforms constitute the primary component cost drivers in floating wind farms. In this specific case study, the transmission system also represents a significant cost component, comprising approximately 16% of the total, attributed to the 50 km distance to shore, highlighting the importance of transmission costs with increasing distance. In general, these findings emphasize the cost distribution within a floating wind farm, with wind turbines and platforms being the main expenses, while the transmission system and O&M are crucial for longer distances to the shore.

Table 8. Breakdown of the costs for a floating offshore wind farm case (* operation and maintenance cost is considering the total lifetime of the wind farm).

	Costs [M€]	Costs per MW [M€/MW]	Costs [%]
Wind turbine cost	1706.25	1.14	19.5
Transmission cost	1028.27	0.69	12.0
Platform cost	1850.37	1.23	21.3
Mooring cost	405.73	0.27	4.6
Anchor cost	353.62	0.24	4.2
Planning, development, and financing	638.35	0.43	7.5
Installation cost	400.96	0.27	4.7
Total CAPEX	**6383.55**	**4.26**	**73.8**
Operation and maintenance *	2278.34	1.51	26.2
Total cost	**8661.89**	**5.77**	**100**

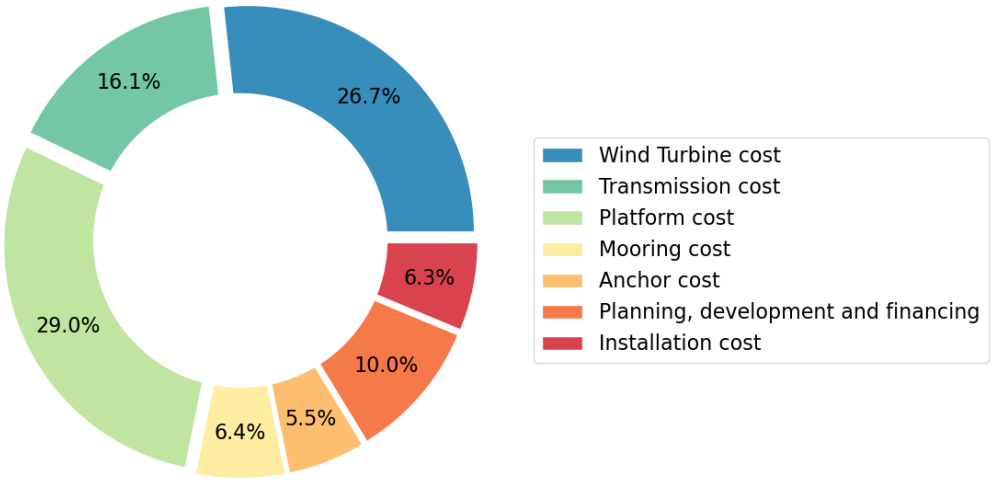

Figure 6. Breakdown of the expenditures (in percentage) for a floating offshore wind farm case.

The diagram in Figure 7 shows how water depth and distance to shore affect costs. With regard to water depth, it is evident that mooring costs increase as anticipated, mainly due to the necessity for longer mooring lines in deeper water. In contrast, while anchor costs also increase, their impact is relatively minor and might not be noticeable in the graph. As expected, OPEX is the parameter that mostly depends on the distance to the shore, increasing at about 25% when going from a near-coast location to a distance of 150 km away from the coastline. The transmission costs also increase with a larger distance to the shore, though not as distinct as expected. This may originate from the model's underestimation of electrical losses over long distances. The increased distance to the shore increases the likelihood of significant electrical losses, potentially requiring the use of shunt reactors to offset capacitive power and a shift towards high-voltage direct current (HVDC) transmission systems. These adjustments could lead to higher transmission costs if included in the model.

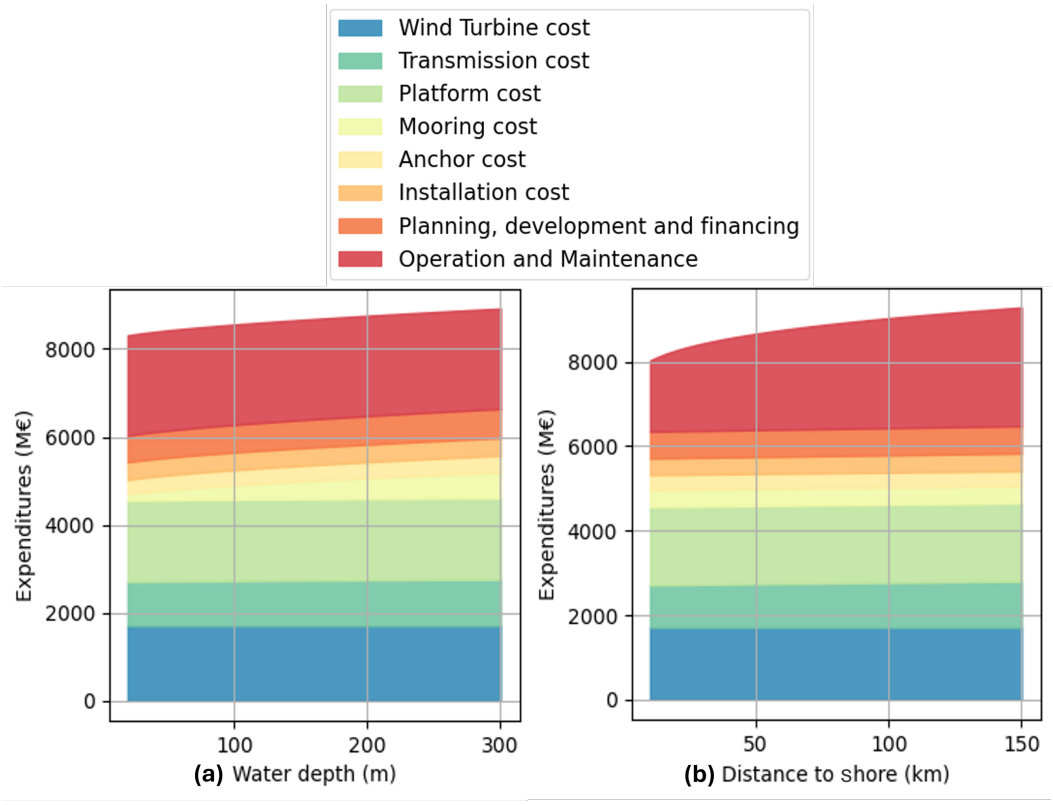

Figure 7. Breakdown of the costs with the influence of (**a**) water depth and (**b**) distance to shore for a floating offshore wind farm case.

3.2. Analysis of Levelized Cost of Energy

The levelized cost of energy is used to compare technology costs and assess economic viability over time. Combining cost and energy production into a single metric determines the minimum selling price of energy needed for project profitability. Using the model described above, with input data from the mapped distributions of Weibull parameters and bathymetry data, the LCoE is mapped across the North Sea for spar and semi-submersible platforms, considering turbine specifications, wind speeds, water depths, and distance to shore. The wind resource data, sourced from the Global Wind Atlas at a hub height of 150 m, required a simple extrapolation and second-order numerical filter to account for missing data of the central North Sea, as detailed in [15]. Water depth data are obtained from the General Bathymetric Chart of the Oceans (GEBCO) following the method described in [42]. Additionally, the distance to shore is computed, corresponding to the Euclidean distance to the nearest point with elevation larger than zero in the GEBCO-treated dataset. As a reference case is chosen a wind farm consisting of 100 15 MW wind turbines located 7 rotor diameters from each other at different locations in the North Sea. To compute the LCoE, the wind farm is expected to have a lifetime of 20 years, and decommissioning expenditures (DECEX) are disregarded. A list of input parameters is given in Table 9, which also refers the different types of substructures (T) to the respective maps of LCoE.

From the isoplots of semi-submersible platforms depicted in Figure 8, LCoE ranges from EUR 9 to 13 cents/kWh, with the highest values near Norway due to deep water and low wind conditions. The central part of the North Sea shows lower LCoE due to shallower waters and higher wind speeds. Similarly, an LCoE range can be observed in the case of spar platforms in Figure 9, which however, is limited to deeper waters (minimum 80 m depth prerequisite for this technology).

Table 9. Input parameters for the LCoE map results.

Parameter	LCoE Map (Figure 8)	LCoE Map (Figure 9)	LCoE Map (Figure 10)
λ	Variable	Variable	Variable
k	Variable	Variable	Variable
A	238 km^2	238 km^2	238 km^2
N_T	100	100	100
P_G	15 MW	15 MW	15 MW
D	245 m	245 m	245 m
h	150 m	150 m	150 m
H	Variable	Variable	Variable
T	Semi-submersible	Spar	Semi-submersible and Bottom-fixed
Y	Variable	Variable	Variable
i	2.2%	2.2%	2.2%
r	5%	5%	5%
Y_O	20 years	20 years	20 years

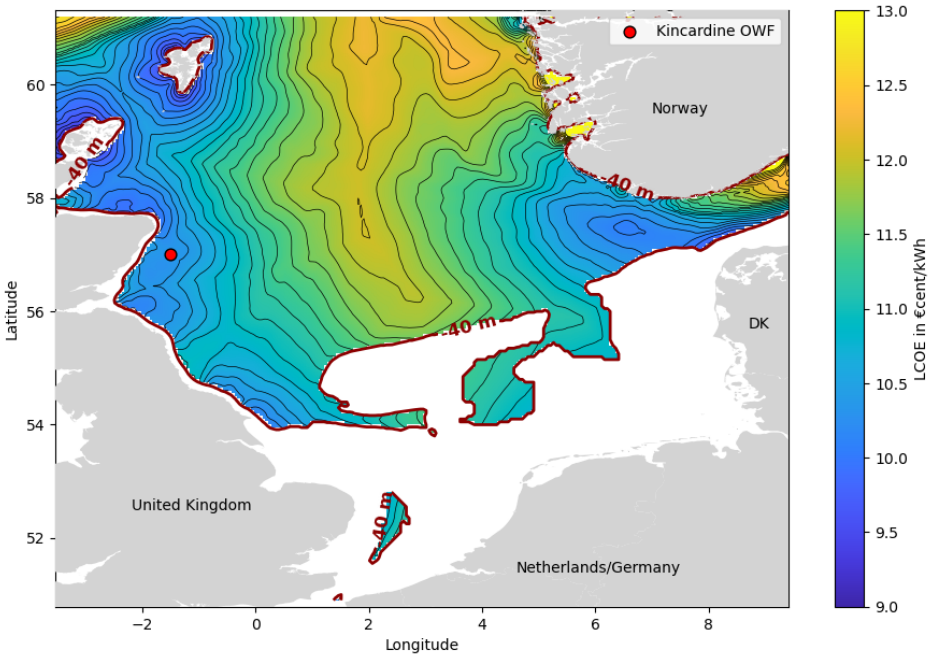

Figure 8. LCoE of a floating **semi-submersible** wind farm, with P_G = 15 MW, D = 245 m, H = 150 m, S = 7, N_T = 100, YO = 20 years, and r = 5%. The red isoline represents a bathymetric depth of −40 m. The red dot corresponds to the *Kincardine* semi-submersible wind farm.

Figure 10 compares the LCoE's for bottom-fixed and floating wind farms, showing the lowest LCoE values associated with bottom-fixed and semi-submersible wind farms. The transition point where floating installations become more economical than fixed ones is mainly determined by the site's bathymetry, typically occurring around a water depth of 55 m. These results are in agreement with the literature, suggesting a transition depth of 50 to 60 m for this kind of high-capacity turbines. Since the foundation cost is the parameter that most differentiates the costs between fixed and floating wind turbines,

a simple test has been conducted to assess the transition between the costs of the two foundation types. Using the same wind farm parameters and conditions as for Horns Rev 2 and 3, respectively, the depth of the water is varied until floating foundations become the most cost-effective. These two wind farms are located close to each other west of the coast of Jutland in Denmark. Horns Rev 2 was commissioned in 2009 with a total installed capacity of 209 MW, and Horns Rev 3 was commissioned in 2019 with an installed capacity of 407 MW. More details about the wind farms are given in Table 10. The results of the test are shown in Figure 11. Hence, according to the model used, Horns Rev 2 would have been more economically efficient as a floating wind farm if the water depths had been deeper than 56.9 m. For Horns Rev 3, a floating wind farm concept would have been the economically most attractive solution at 51.4 m. It is worth noting that the sudden change in the fixed-bottom cost curve is caused by the transition from monopile to jacket technology, which becomes necessary because monopiles are assumed to be unsuitable for depths of more than 35 m, as explained in [14]. Unfortunately, because of lack of reference data, it is not possible to validate the computed LCoE values, even less the uncertainty on these. The lack of data is partly due to confidentiality and partly due to the lack of knowledge regarding the costs of maintaining floating wind farms. However, as a guideline, in our previous work on fixed-bottom offshore wind farms, CAPEX and annual power production were on average determined within 5%, as compared with actual performance and cost data.

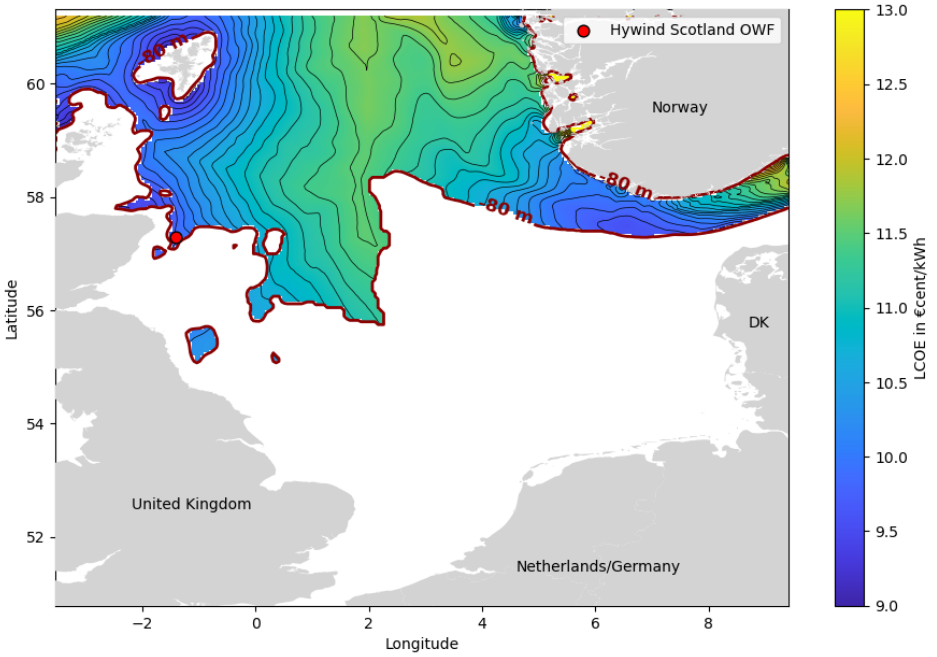

Figure 9. LCoE of a floating **spar** wind farm, with P_G = 15 MW, D = 245 m, H = 150 m, S = 7, N_T = 100, Y_O = 20 years, and r = 5%. The red isoline represents a bathymetry depth of 80 m. The red dot corresponds to the *Hywind Scotland* spar wind farm.

Note that the size of the wind turbines has an influence on the results, with these two real cases consisting of smaller turbines than the computations presented in Figure 10. Hence, as expected, while bottom-fixed wind farms are more cost-effective in shallow waters, floating wind farms become viable at larger depths, with ongoing technological advancements expected to reduce their costs over time.

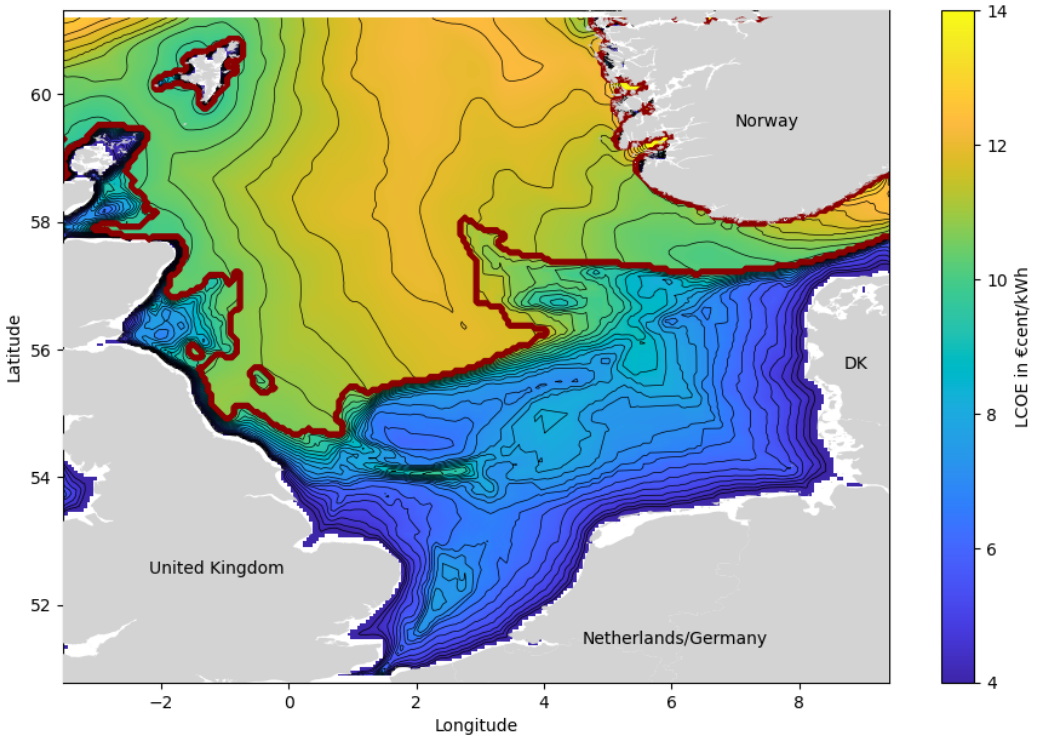

Figure 10. Comparison of LCoE's between a floating semi-submersible wind farm and a bottom-fixed wind farm, with P_G = 15 MW, D = 245 m, H = 150 m, S = 7, N_T = 100, Y_O = 20 years, and r = 5%. The red line indicates the transition from bottom-fixed to floating wind farms.

Table 10. Input parameters to the LCoE analysis on Horns Rev 2 and Horns Rev 3 with variable water depth.

Parameter	LCoE on HR2 (Figure 11 Left)	LCoE on HR3 (Figure 11 Right)
λ	11.2	11.5
k	2.4	2.4
A	33.6 km^2	83.3 km^2
N_T	91	49
P_G	2.3	8.3
D	93	164
h	68	105
H	Variable	Variable
T	All	All
Y	32 km	22 km
i	2.2%	2.2%
r	5%	5%
Y_O	20 years	20 years

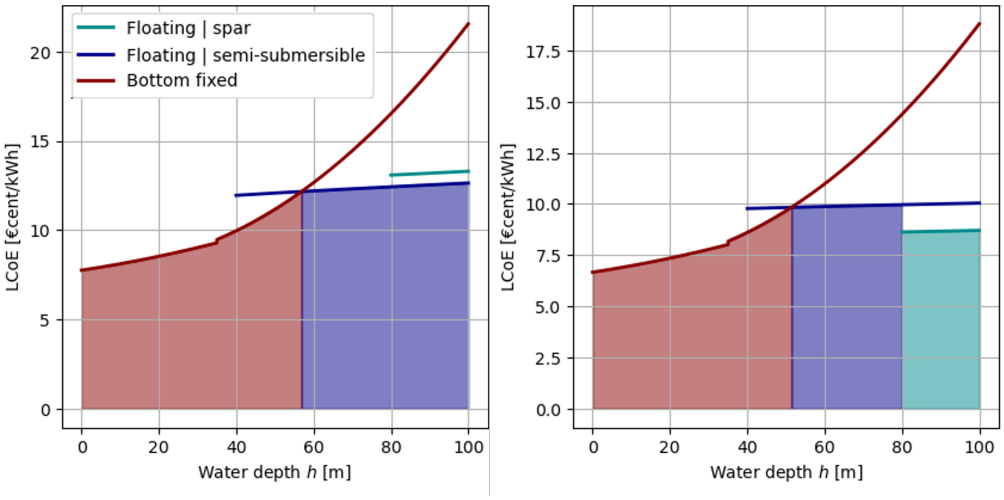

Figure 11. Variation of the LCoE with water depth at the location of Horns Rev 2 (**left**) and Horns Rev 3 (**right**).

4. Conclusions

A simple techno-economic model is proposed to determine costs related to the development of floating offshore wind power. The model is an extension of the minimalistic prediction model for fixed-bottom wind farms previously developed by Sørensen and Larsen [14]. In the extended version, cost components associated with the deployment of floating structures, such as floaters, mooring lines, anchors, and additional installation and operational expenses, are included. The platform cost is determined using scaling laws that link the turbine's total mass and rated capacity multiplied by the material's mass cost. It is noted that the platform cost estimation is subject to uncertainty due to the wide range of possible scaling laws and the use of fictive studies or prototypes as data sources. The costs of mooring lines and anchors are derived from catenary equations combined with literature-based line tension and cost information.

Different types of floaters, mooring line systems, and anchors are addressed and subsequently synthesized with actual wind climate and bathymetric data for the North Sea to map the annual energy production and LCoE for floating wind farms located in this sea regime. The analysis includes aspects of varying distances to the shore as well as the water depths, thus allowing for a thorough examination of their impacts on the overall costs of floating wind. The North Sea demonstration case shows—as expected—that floating wind farms are less affected by water depth than bottom-fixed installations, and that turbines and floater platforms are the primary component cost drivers in floating wind farms. The transition point where floating installations are more economical than fixed installations is mainly determined by the site's bathymetry, typically occurring around a water depth of 55 m. Interestingly, this result is in agreement with the literature, suggesting a transition depth of 50 to 60 m for high-capacity turbines.

While the proposed model provides a simple approach to estimate costs specific to floating offshore wind power, it was not feasible to fully adapt certain cost equations from fixed-bottom installations to floating systems. For instance, while the wind turbine cost equations appear to require minimal adjustments due to relatively small differences between fixed-bottom and floating systems, OPEX can vary significantly. This is because the floating wind industry does not yet have a standardized approach to O&M; instead, new methods are still being tested in prototype projects. These variations in O&M strategies, including access methods and maintenance schedules, contribute to a lack of reliable data and introduce uncertainty into the analysis. Future work should focus on collecting empirical data from operational floating wind projects, not only to refine OPEX modeling

but also to validate the assumptions and extrapolations made for other components of floating wind farms, ensuring the accuracy of cost estimates across all parameters.

Author Contributions: A.M.: conceptualization, methodology, software, validation, formal analysis, investigation, resources, writing—original draft preparation, writing—review and editing, visualization. D.F.: conceptualization, methodology, software, validation, formal analysis, investigation, writing—original draft preparation, writing—review and editing, visualization. J.N.S.: conceptualization, methodology, software, validation, formal analysis, investigation, resources, writing—original draft preparation, writing—review and editing, supervision, project administration, funding acquisition. G.C.L.: conceptualization, methodology, formal analysis, investigation, writing—original draft preparation, writing—review and editing, supervision, project administration. All authors have read and agreed to the published version of the manuscript.

Funding: This study is partly funded by the European Union through the Horizon Europe project INF^{4}INiTY under Grant Agreement No. 101136087.

Data Availability Statement: All data cited and used as input to the model and the presented results are publicly available and can be found in the open literature.

Conflicts of Interest: The authors declare no conflicts of interest.

Abbreviations

Name	Symbol	Units
Annual power production	P_E	MW
Average annual power yield of a solitary turbine	$P_{WF,y}$	Wh
Capacity factor	C_f	-
Chain cost per unit of mass	c_{ML}	€/kg
Correction constant (finite farms)	a	-
Cost of array cables	C_{ac}	M€
Cost of export cables	C_{ec}	M€
Cost of operation and maintenance	$C_{O\&M}$	M€
Cost of the electrical transmission system	C_{TS}	M€
Cost of the offshore substation	C_{off-s}	M€
Cut-in wind speed	U_i	m/s
Cut-out wind speed	U_o	m/s
Mean wind speed	U	m/s
Gravitational acceleration	g	m/s^2
Geostrophic wind speed	G	m/s
Inflation rate	r	-
Inter-array cable length	L_I	km
Inter-turbine spacing	S	-
Length of mooring line	l	m
Mass of chain per unit of length	m_{ML}	kg/m
Mass of the reference floating platform	m_{ref}	kg
Mass of the scaled floating platform	m_{scaled}	kg
Mean production in free wind speed	P_{Free}	Wh
Mooring element section area	A_s	m^2
Mooring lines cost	C_{ML}	M€
Mooring line installation cost	$C_{i,ML}$	M€
Number of anchors	$N_{anchors}$	-
Number of mooring lines	N_{ML}	-
Number of turbines	N_T	-
Rated power	P_G	MW
Rated power of the reference wind turbine	P_{ref}	W
Rated power of the scaled wind turbine	P_{scaled}	W

Rated thrust coefficient	$C_{T,r}$	-
Rated wind speed	U_r	m/s
Rotor diameter	D	m
Scale parameter (Weibull)	λ	m/s
Shape parameter (Weibull)	k	-
Tension of the mooring line at the anchor point	T_{anchor}	N
Transmission system installation cost	$C_{i,TS}$	M€
Turbine and semi-sub foundation installation cost	$C_{i,WT-semisub}$	M€
Turbine and spar foundation installation cost	$C_{i,WT-spar}$	M€
Turbine cost	C_{WT}	€
Turbine thrust impact parameter	c_t	-
Von Kármán constant	κ	-
Water density	ρ_{water}	kg/m^3
Water depth	H	m
Wind farm area	A	m^2
Wind farm density	d_{WF}	MW/km^2
Wind speed at hub height	U_h	m/s
Years of operation of the wind farm	Y_O	years

References

1. Number of Wind Farms in EU. Available online: https://www.statista.com/statistics/666495/number-of-windfarms-eu/ (accessed on 5 July 2024).
2. Yang, R.; Chuang, T.; Zhao, C.; Johanning, L. Dynamic Response of an Offshore Floating Wind Turbine at Accidental Limit States—Mooring Failure Event. *Appl. Sci.* **2022**, *12*, 1525. [CrossRef]
3. Ma, K.T.; Luo, Y.; Kwan, T.; Wu, Y. *Mooring System Engineering for Offshore Structures, Chapter 2—Types of Mooring Systems*; Elsevier: Amsterdam, The Netherlands, 2019.
4. Jump, E. Mooring and Anchoring Systems—Market Projections. 2021. Available online: https://cms.ore.catapult.org.uk/wp-content/uploads/2021/12/PN000413-RPT-003-Rev-2-Mooring-and-Anchoring-Market-Projections_Formatted.pdf (accessed on 6 February 2023).
5. Ernst & Young. *Cost of and Financial Support for Offshore Wind*; Technical Report, Department of Energy and Climate Change; Ernst & Young: London, UK , 2009.
6. EWEA. Wind Energy—The Facts, Chapter 2 (Economics): Offshore Developments, The Cost of Energy Generated by Offshore Wind Power. Technical Report, EWEA. 2009. Available online: https://www.wind-energy-the-facts.org/index-44.html (accessed on 23 January 2023).
7. Morthorst, P.; Kitzing, L. Economics of building and operating offshore wind farms. In *Offshore Wind Farms*, 1st ed.; Ng, C., Ran, L., Eds.; Number 92 in Woodhead Publishing Series in Energy; Woodhead Publishing: Amsterdam, The Netherlands, 2016; pp. 9–28.
8. Gonzalez-Rodriguez, A.G. Review of offshore wind farm cost components. *Energy Sustain. Dev.* **2017**, *37*, 10–19. [CrossRef]
9. Castro-Santos, L.; Filgueira-Vizoso, A.; Lamas-Galdo, I.; Carral-Couce, L. Methodology to calculate the installation costs of offshore wind farms located in deep waters. *J. Clean. Prod.* **2018**, *170*, 1124–1135. [CrossRef]
10. Ioannou, A.; Brennan, F. A preliminary techno-economic comparison between a grid-connected and non-grid connected offshore floating wind farm. In Proceedings of the 2019 Offshore Energy and Storage Summit, OSES, Brest, France, 10–12 July 2019.
11. Lozer dos Reis, M.M.; Mitsuo Mazetto, B.; Costa Malateaux da Silva, E. Economic analysis for implantation of an offshore wind farm in the Brazilian coast. *Sustain. Energy Technol. Assess.* **2021**, *43*, 100955. [CrossRef]
12. Castro-Santos, L.; Silva, D.; Bento, A.R.; Salvação, N.; Soares, C.G. Economic feasibility of floating offshore wind farms in Portugal. *Ocean Eng.* **2020**, *207*, 107393. [CrossRef]
13. Martinez, A.; Iglesias, G. Mapping of the levelised cost of energy for floating offshore wind in the European Atlantic. *Renew. Sustain. Energy Rev.* **2022**, *154*, 111889. [CrossRef]
14. Sørensen, J.N.; Larsen, G.C. A Minimalistic Prediction Model to Determine Energy Production and Costs of Offshore Wind Farms. *Energies* **2021**, *14*, 448. [CrossRef]
15. Sørensen, J.N.; Larsen, G.C.; Cazin-Bourguignon, A. Production and Cost Assessment of Offshore Wind Power in the North Sea. Wake Conference; IOP Publishing: Visby, Sweden, 2021; Volume 1934. [CrossRef]

16. Sørensen, J.N.; Garcia, A.; Larsen, G.C.; Pedersen, M.M.; Fournely, D. Extension and Validation of Minimalistic Prediction Model to Determine the Energy Production of Offshore Wind Farms. In Proceedings of the Science of Making Torque from Wind: Wind Resource, Wakes, and Wind Farms, Torque, Firenze, Italy, 29–31 May 2024. [CrossRef]
17. Frandsen, S. On the wind speed reduction in the center of large clusters of wind turbines. *J. Wind Eng. Ind. Aerodyn.* **1992**, *39*, 251–265. [CrossRef]
18. Frandsen, S.; Barthelmie, R.; Pryor, S.; Rathmann, O.; Larsen, S.; Hojstrup, J.; Thogersen, M. Analytical modelling of wind speed deficit in large offshore wind forms. *Wind Energy* **2006**, *9*, 39–53. [CrossRef]
19. Leimeister, M.; Kolios, A.; Collu, M. Critical review of floating support structures for offshore wind farm deployment. *J. Phys. Conf. Ser.* **2018**, *1104*. [CrossRef]
20. Vryhof Anchors B.V. Anchor Manual 2015: The Guide to Anchoring. Available online: https://www.plaisance-pratique.com/IMG/pdf/Vryhof_Anchor_Manual2015.pdf (accessed on 6 February 2023).
21. Benassai, G.; Campanile, A.; Piscopo, V.; Scamardella, A. Optimization of Mooring Systems for Floating Offshore Wind Turbines. *Coast. Eng. J.* **2015**, *57*, 1550021.
22. Sergiienko, N.; da Silva, L.; Bachynski-Polić, E.; Cazzolato, B.; Arjomandi, M.; Ding, B. Review of scaling laws applied to floating offshore wind turbines. *Renew. Sustain. Energy Rev.* **2022**, *162*, S1364032122003811. [CrossRef]
23. The World Bank. Inflation Consumer Prices. Available online: https://data.worldbank.org/indicator/FP.CPI.TOTL.ZG?end=2022&start=1960 (accessed on 15 April 2023).
24. Maienza, C.; Avossa, A.; Ricciardelli, F.; Coiro, D.; Troise, G.; Georgakis, C. A life cycle cost model for floating offshore wind farms. *Appl. Energy* **2020**, *266*, 114716. [CrossRef]
25. BVG Associates. Guide to an Offshore Wind Farm. 2019. Available online: https://www.thecrownestate.co.uk/media/2860/guide-to-offshore-wind-farm-2019.pdf (accessed on 5 January 2023).
26. Stehly, T.; Duffy, P. 2021 Cost of Wind Energy Review. 2022. Available online: https://www.nrel.gov/docs/fy23osti/84774.pdf (accessed on 21 January 2023).
27. Siemens Gamesa. Siemens Gamesa Activity Report—Year 2022. Available online: https://www.siemensgamesa.com/global/en/home/press-releases/111022-siemens-gamesa-press-release-results-presentation-q4-fy2022.html (accessed on 24 March 2023).
28. Vestas. Vestas Annual Report. 2022. Available online: https://www.vestas.com/en/media/company-news/2023/vestas-annual-report-2022---a-challenging-year-with-neg-c3710817 (accessed on 24 March 2023).
29. Huang, Q.; Wang, X.; Fan, J.; Zhang, X.; Wang, Y. Reliability and economy assessment of offshore wind farms. *J. Eng.* **2019**, *2019*, 1554–1559. [CrossRef]
30. Pricing Tool for the "New Continuum". Available online: http://steelbenchmarker.com/ (accessed on 15 April 2023).
31. Innovative Concepts for Floating Structures. 2014. Available online: http://www.innwind.eu/ (accessed on 13 January 2023).
32. Faltinsen, O.M. *Sea Loads on Ships and Offshore Structures*; Cambridge University Press: Cambridge, UK, 1990.
33. Xu, K.; Larsen, K.; Shao, Y.; Zhang, M.; Gao, Z.; Moan, T. Design and comparative analysis of alternative mooring systems for floating wind turbines in shallow water with emphasis on ultimate limit state design. *Ocean Eng.* **2021**, *219*, 108377. [CrossRef]
34. Kim, H.; Young Jeon, G.; Choung, J.; Yoon, S.W. Study on Mooring System Design of Floating Offshore Wind Turbine in Jeju Offshore Area. *Int. J. Ocean Syst. Eng.* **2013**, *3*, 209–217. [CrossRef]
35. Connolly, P.; Hall, M. Comparison of pilot-scale floating offshore wind farms with shared moorings. *Ocean Eng.* **2019**, *171*, 172–180. [CrossRef]
36. Figueiredo, P.; Brójo, F. Parametric study of multicomponent mooring lines at catenary form in terms of anchoring cost. *Energy Procedia* **2017**, *136*, 456–462. [CrossRef]
37. Hall, M.; Lozon, E.; Housner, S.; Sirnivas, S. Design and analysis of a ten-turbine floating wind farm with shared mooring lines. *J. Phys. Conf. Ser.* **2022**, *2362*, 012016. [CrossRef]
38. Karimi, M.; Hall, M.; Buckham, B.; Crawford, C. A multi-objective design optimization approach for floating offshore wind turbine support structures. *J. Ocean Eng. Mar. Energy* **2017**, *3*, 69–87. [CrossRef]
39. Cabioch, K. Improvement of Wind-Resource/Cost Model for Offshore Wind Farms. Master's Thesis, DTU Wind Energy, Technical University of Denmark, Roskilde, Denmark, 2022.
40. Danish Energy Agency. Offshore Wind Potential in the North Sea. 2022. Available online: https://ens.dk/media/2414/download (accessed on 30 January 2023).
41. Centeno-Telleria, M.; Yue, H.; Carrol, J.; Penalba, M.; Aizpurua, J.I. Impact of operations and maintenance on the energy production of floating offshore wind farms across the North Sea and the Iberian Peninsula. *Renew. Energy* **2024**, *224*, 120217. [CrossRef]
42. GEBCO. General Bathymetric Chart of the Oceans. Available online: https://www.gebco.net/ (accessed on 2 March 2023).